Finite-element simulations of the punching tests on shear-retrofitted slab-column connections

A. Negele, R. Eligehausen & J. Ožbolt
Institute of Construction Materials, Universitaet Stuttgart, Germany

M. A. Polak
Department of Civil and Environmental Engineering, University of Waterloo, Canada

ABSTRACT: A new type of shear reinforcement, shear bolts, are used for retrofit and strengthening of existing previously built concrete slabs to increase the punching capacity. The bolts are installed in holes drilled in a slab in concentric perimeters around the column. The test results showed a load increase up to flexural failure of the slabs and a significantly improved ductility when using shear bolts. The punching tests were investigated using the 3D nonlinear finite-element code MASA which was developed at the Institute of Construction Materials of the Universitaet Stuttgart. The paper discusses the modeling of slabs with shear reinforcement. A proper idealization of the shear reinforcement is essential for the accuracy of the finite-element simulations. The finite-element simulations show good agreement with the test results and give a more detailed insight in the failure mechanism. The models build the basis for an extensive parametric study on the punching behavior of flat slabs.

1 INTRODUCTION

Flat slabs are widely used in reinforced concrete constructions. The connections between columns and slabs are subject to high stresses which might lead to a brittle punching shear failure. To increase the punching shear capacity and the ductility of the slab-column connections shear reinforcement can be used. Conventional shear reinforcements such as stirrups, bent up bars and shear studs are installed before casting of the concrete. Shear studs have been proved to be the most effective and easy to install shear reinforcement (e.g. Dilger & Ghali 1981).

Changes in the building use, the need of installing new services and construction or design errors might require strengthening of existing slabs. Therefore, a simple and effective method for subsequent installation of shear reinforcement was developed. These shear bolts consist of a rod with a head at one side and a thread at the other side. The shear bolts are slid in drilled holes and fixed with a washer and nut system at the threaded end. With this system the bolts are supplied with a comparatively stiff anchorage system as shear studs.

Tests on slab column connections of interior and edge slab column connections (Adetifa & Polak 2005, El-Salakawy et. al. 2003) show a load increase up to flexural failure of the slab column connections and a considerable increase in ductility.

For a better understanding of the punching failure and as a basis for parametric studies, the tests on interior slab column connections were modeled using the finite element method. In the following the modeling of the slabs and the results of the finite element simulations with the program MASA are presented.

2 PUNCHING TESTS

A series of four punching tests on interior slab-column connections was used for the finite element study. A detailed description of the tests can be found in Adetifa & Polak (2005).

2.1 *Test Setup and Parameters*

All tests were performed on square slabs with side lengths of 1800mm and a thickness of 120mm. The loading was applied on square column stubs with cross sections of 150 x 150mm. The test parameters can be found in Table 1.

Table 1. Test Parameters

Spec.	SB rows	s_0	s_i	bolt Ø [mm]	thick-ness h [mm]	depth d [mm]	flexural reinf. ρ [%]
SB1	0	-	-	-	120	90	1.25
SB2	2	0.56d	0.89d	9.5	120	90	1.25
SB3	3	0.56d	0.89d	9.5	120	90	1.25
SB4	4	0.56d	0.89d	9.5	120	90	1.25

SB: shear bolts

The main test parameter was the number of shear bolts. A slab reinforced with two rows of shear bolts is shown in Figure 1. The distance of the first shear bolt to the column was s_0=50mm all other rows were spaced at s_i=80mm (Table 1). The bolts were placed in a cross shape with two bolts on each column face. They were installed in drilled holes with a diameter of 16mm. Washers with a diameter of 44mm and thicknesses of 10mm were used. The nuts were torqued hand tight before testing. The flexural tension reinforcement consisted of 10M bars (A=100mm²) with 90mm and 100mm spacing for the top and bottom layers, respectively.

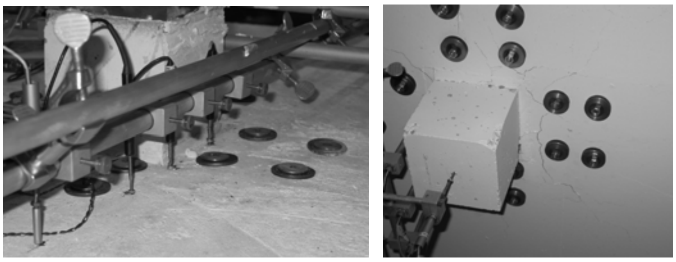

Figure 1. Strengthened slab with shear-bolts.

All slabs were simply supported along the edges at a distance of 1500mm; the corners were restraint to avoid lifting up (Figure 2). The simple support was realized through 40mm wide steel plates with Neoprene strips to allow rotations at the supports.

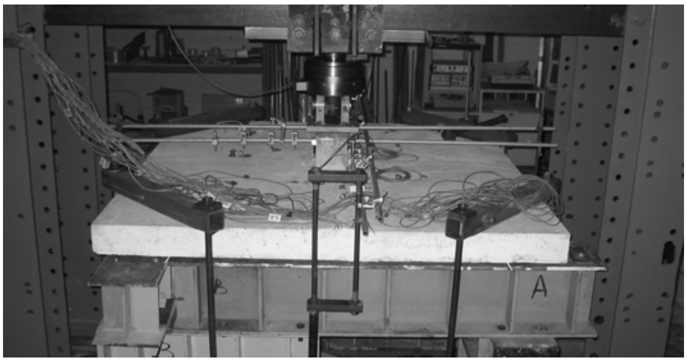

Figure 2. Experimental setup with test specimen.

2.2 *Test Results*

The slab without shear reinforcement failed in punching. Specimen SB2 failed in a combined failure mode of punching outside the shear bolts and flexure. All other slabs failed in flexure. The slabs show a distinct flexural crack on the tension side of the slab between the column face and the first row of shear bolts. After a considerable yield plateau a shear crack occurred outside the shear reinforced zone. The shear crack is clearly visible on the compression side of the slab. On the tension side the shear crack is partly visible. This is due to the fact that the shear crack runs along the tensional flexural reinforcement and does not directly protrude through the slab. The test results are summarized in Table 2, typical crack development is shown in Figure 3. More detailed results are discussed in chapter 4.

Table 2. Test results

Spec.	SB rows	$f_{c,cyl}$ [MPa]	Failure load [kN]	Displ. [mm]	Mode
SB1	0	44	253	12	P
SB2	2	41	364	28	P/F
SB3	3	41	372	33	F
SB4	4	41	360	48	F

SB: shear bolts
Displ.: Column displacement at failure load
Mode: P - Punching, F- Flexural Failure

a) compression side b) tension side
Figure 3. SB3 –crack development after testing.

3 FINITE-ELEMENT CODE AND MODELING

The finite-element simulations were performed with the three-dimensional nonlinear finite-element code MASA. This code was developed at the Institute of Construction Materials at the Universitaet Stuttgart. The finite element code MASA is designed for the nonlinear analysis of quasi-brittle materials such as concrete.

3.1 *MASA fundamentals*

The finite element code MASA is based on the mircroplane material model with relaxed kinematic constraint (Ožbolt et al. 2001). In numerous investigations it has been shown that MASA is able to predict the behavior of reinforced concrete structures and the punching failure of flat slabs realistically (Ožbolt et al. 1999, Beutel 2002). The program uses a smeared crack approach in combination with the crack band method as a localization limiter (Ožbolt & Bažant 1996).

3.2 *Modeling with three-dimensional elements*

Concrete or massive steel members are modeled with three dimensional elements. Hexahedra elements result in simple meshes with relatively few elements. Tetrahedral elements allow the meshing of arbitrary geometries and are therefore used more often. Principally bar reinforcement can also be modeled with three dimensional elements. However, in large scale structures the reinforcement needs to be simplified with one dimensional truss elements.

3.3 *Modeling of reinforcement with bar elements*

Reinforcement bars can be modeled with one dimensional bar elements. Bar elements have a real length and a defined cross section. An additional virtual length that is used for calculating the bending stiffness in the finite element program allows controlling the flexural rigidity of the elements. Bar elements share their end nodes with the adjacent three-dimensional concrete elements, which results in a fixed connection between both elements.

3.4 *Modeling of reinforcement with bond elements*

In all cases were the bond behavior of the reinforcement influences the load bearing behavior considerably. The use of bond elements gives more realistic results of the finite element simulations. A bond element is an additional two node spring element that connects the end node of a bar element with the adjacent node of the concrete elements (Figure 4). The bond element is defined by a bond-slip curve and realizes the load transfer between the bar element and the concrete elements according to this definition. The development of the bond element and the implementation of bond-slip curves for standard deformed reinforcement bars can be found in Lettow et al. (2004) and Lettow (2006).

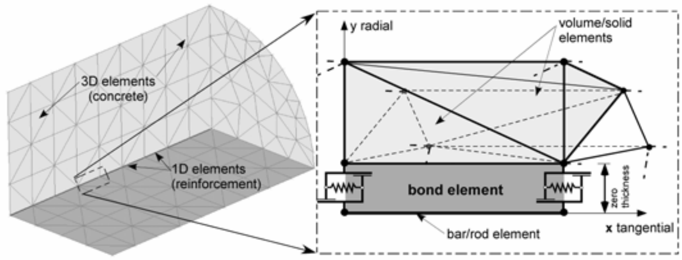

Figure 4. Definition of the bond element.

3.5 *Modeling of anchorage elements*

When bar or bond elements are used to model headed bars, stirrups or hooked bars the anchorage element must also be idealized by bar or bond elements. The anchorage element can be idealized applying two different methods. The first option is to arrange the bar elements in a cross or hook shape (Figure 5 a, b). The anchorage slip of the idealized head is controlled by introducing a virtual element length for the calculation of the internal flexural element stiffness. The stiffness can be calibrated on finite-element pull-out tests. A representative slip is computed using equation (1) for head slip; it depends on the head pressure (Furche 1994):

$$s = \frac{k_A}{c} \cdot \left(\frac{\sigma}{f_c} \right)^2 \tag{1}$$

$$k_A = 0.5 \cdot \sqrt{d_s^2 + 9 \cdot (d_k^2 - d_s^2)} - d_k / 2 \tag{2}$$

s: head slip
d_k: head diameter
d_s: shaft diameter
k_A: factor for influence of head-shaft ratio
σ: head pressure
c=600 for uncracked concrete
c=300 for cracked concrete
f_c: concrete strength, 200mm cube

It must be noted that the forces that can be transmitted when a bar element is anchored in cracked concrete elements are very small. Therefore, in such case the number of elements for the head must be increased (tension side of a flat slab, Figure 5 c). However, elements with a large flexural stiffness might influence the flexural behavior of the whole structure or lead to local damage if they are used in regions with high local deformations. Therefore, the second modeling option is to use bar elements with a flexible joint and arrange them in a truss shape to provide the anchorage (Figure 5 d). With this option a rotation of the head is possible and the damage is minimized. The disadvantage of this solution is that the slip behavior of the anchorage element cannot be directly controlled. Furthermore, the modeling depends on a regular finite element mesh as shown in Figure 5d.

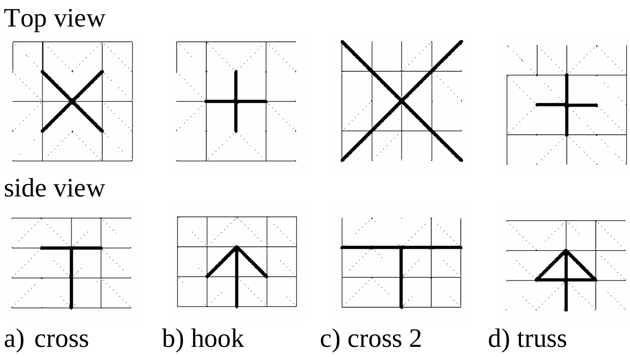

Figure 5. Anchorage of bar elements.

Preliminary studies have shown that for anchorage in severely cracked concrete, as in the case of the bending cracks of a slab, a large cross as shown in Figure 5 c needs to be applied to ensure adequate anchorage. In regions with large deformations and without flexural cracks, as can be found on the bottom side of the slab, especially close to the column, truss elements as shown in Figure 5 d should be used.

4 FINITE-ELEMENT SIMULATIONS

In the finite-element simulations, a symmetrical slab can be modeled by a quarter of a slab. All nodes along symmetry planes need to be fixed in the direction orthogonal to the plane to account for symmetry.

4.1 *Model of the slab*

The slab is modeled with column stubs on both sides of the slab. The concrete is modeled with tetrahedral elements with an element size of approximately 14mm. A section of the quarter of the slab is shown in Figure 6a. It shows a view on the tension side of the slab column connection. The modeling of a shear bolt is shown in Figure 6b. The bolt is modeled according to section 3.5 with bond elements with a defined flexural stiffness on the tension side of the slab, and bond elements as a truss on the compression side of the slab. The sum of the mechanical and frictional bond is set to 0.2N/mm² to simulate the post installed shear bolts with no friction along the drilled hole. The flexural reinforcement is modeled with bar elements; the layout is according to the reinforcement layout in the tests.

The load is applied on the column stub, in displacement controlled mode.

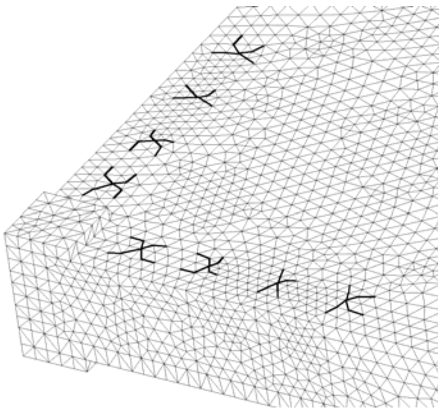

a) Slab section with column stub

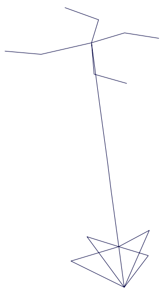

b) Shear bolt

Figure 6. Model of the slab.

4.2 *Material Properties*

The concrete and steel material properties were used according to the material test results of the punching tests, as shown in Table 3. The stress-strain curve for steel was modeled as a trilinear function with yield at 2.3‰ strain reaching ultimate stress at 5% strain.

Table 3. Material properties

Spec.	Concrete $f_{c,cyl}$ [MPa]	$f_{c,t}$ [MPa]	G_f [N/mm]	E_c [MPa]	Steel f_y [MPa]	f_t [MPa]	E_S [MPa]
SB1	44	2.2	0.07	28000	455	650	197000
SB2-4	41	2.1	0.07	28000	455	650	197000

$f_{c,cyl}$: concrete compressive cylinder strength
$f_{c,t}$: concrete tensile strength
G_f: concrete fracture energy
E_c: concrete modulus of elasticity
f_y: steel yield strength
f_t: steel ultimate strength
E_S: steel modulus of elasticity

The concrete at the highly stressed compressive zone at the column face is loaded in a multiaxial state of stress, which results in an increased compressive strength. For slabs with shear reinforcement this strength is further increased by the additional restraint of the compressive zone by the heads of the first studs. This mechanism contributes the ultimate load increase in tested slabs. However, the modeling of shear reinforcement with two dimensional bar or bond elements in finite element simulations does not result in an increased concrete strength at the column face. This needs to be compensated in the simulations by introducing a region with increased concrete strength in the compressive zone at the column face. To account for the increase in the concrete strength, the concrete in that region is modeled with a reduced Poisson’s ratio.

4.3 *Modeling of support conditions*

The vertical supports are realized by restraing of the nodes at a support point or along a support line. In the following simulations the line support of the test is simplified to a radial point support. This better represents the actual test support conditions which are never perfectly restrained and allow some movement.

4.4 *Load-displacement curves*

The punching tests with slabs without and with shear reinforcement show a considerable load increase when shear reinforcement is used (Figure 7). Furthermore the ductility is increased with the number of rows of shear bolts.

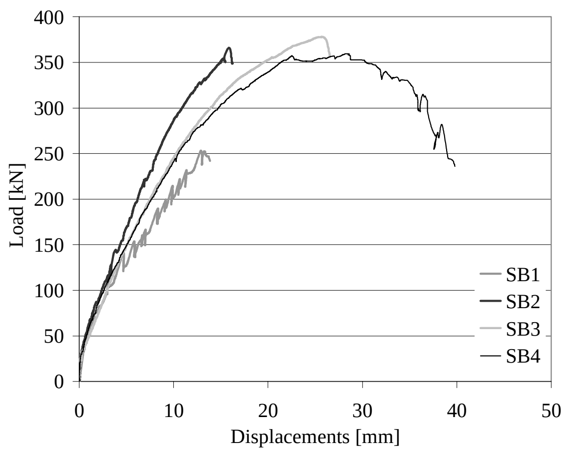

Figure 7. Load displacement curves tests.

The results of the finite-element simulations (Figure 8) show a good agreement with the experimental values of the ultimate loads. Simulation SB1 shows a brittle failure as in the test. For all other tests the ductility is increased considerably. However, the simulations do not show the same large influence of the number of bolts on the ductility as the tests.

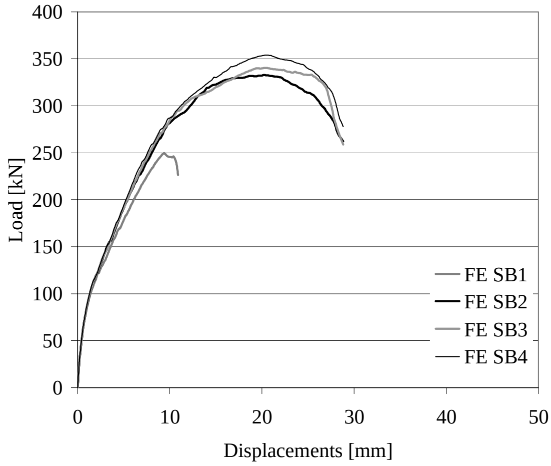

Figure 8. Load displacement curves simulations.

4.5 *Cracking*

The crack development in the finite-element simulations can be visualized through the principal tensile strains in the concrete. The cracking is shown at two sections through the slab. Section 1 is parallel to the y-axis at a distance of 45 mm from the axis. The section cuts one row of shear bolts. Section 2 lies in the slab diagonal where no shear bolts are used. The black shaded areas with maximum strains of 0.03 represent a crack width of 0.4mm for elements with a side length of 14mm. The different strain values are shown at steps of 0.005. The support points are visualized by black triangles.

The crack development of Slab SB1, without shear reinforcement, is shown in Figure 9. The sections show an inclined shear crack of about 37° at section 1 and of about 46°, 32° and 20° at section 2. A direct comparison to the crack development in the test is not possible since the test specimens were not saw cut after testing. A variation of the failure crack angle along the column perimeter has also been reported by Clauss & Birkle (2002). A flexural crack at the face of the column is clearly visible.

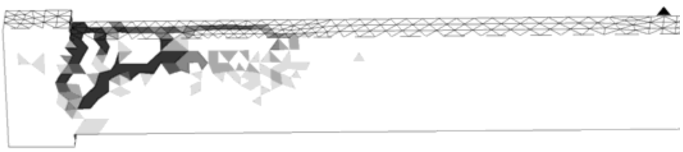

a) slab section 1

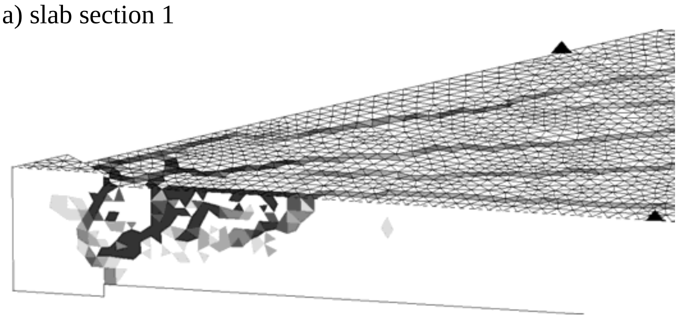

b) slab diagonal

Figure 9. Cracking at ultimate load: SB1.

Figure 10a shows the crack development for a slab with shear reinforcement, SB4, along section 1. The crack development shows a distinct bending crack at the column face beginning on the tension side of the slab as observed in the tests. Outside the shear reinforcement there is a visible shear crack, which was the failure crack in the test. The region between the first and second row of studs is cracked. This might be caused by the influence of the stiff anchorage elements of the shear bolts. This additional cracking influences the ductility of the load displacement curves and leads to a second post failure shear crack between the first two rows of bolts.

The finite-element simulation gives the opportunity to visualize vertical and horizontal strains corresponding to shear and flexural cracking, respectively. Figure 10b shows the horizontal strains along the axis parallel to the slab section. The main crack is the flexural crack at the column face; minor flexural cracking occurs between the first two rows of studs. Figure 10c shows the vertical cracking. The vertical part of shear crack outside the shear reinforcement is clearly visible. The shear crack angle is about 40°. Additionally there are minor vertical strains between the first two shear bolts adjacent to the column.

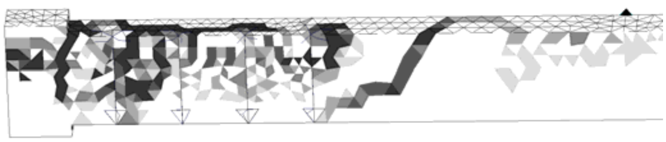

a) Principal tensile strains

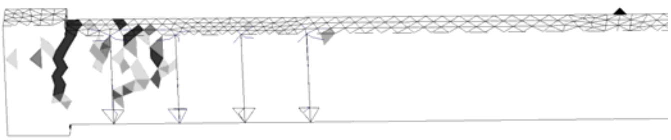

b) Tensile strains in x-direction - flexural cracks

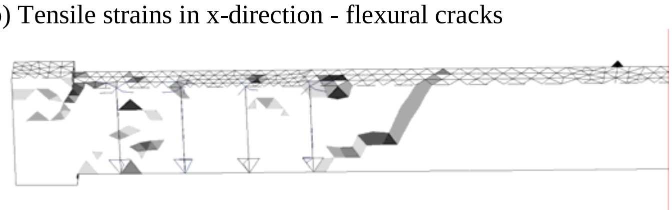

c) Tensile strains in z-direction – shear cracks

Figure 10. Cracking at ultimate load: SB4 section 1.

Section 2 through the slab diagonal shows considerably more shear cracking than the section parallel to the y-axis. This is due to the orthogonal distribution of the shear bolts. The shear crack angles are about 48°, 41°, 25° and 15°. Comparing the crack development on the slab diagonal with the cracking of the slab without shear reinforcement, SB1, it can be observed that the first three cracks are slightly steeper but otherwise similar to the cracks of slab SB1. The additional shallow crack develops at about 90% of the ultimate load. This is the continuation of the crack that develops outside the shear reinforced zone in section 1 and becomes the failure crack in the test.

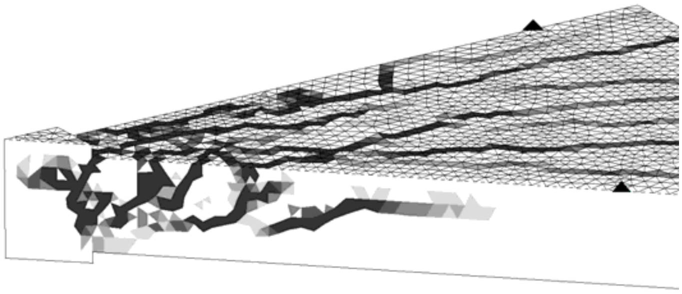

a) Principal tensile strains

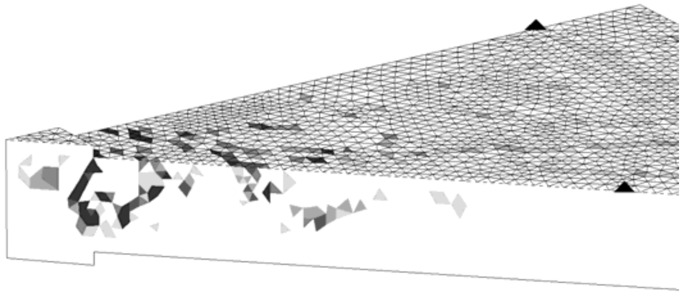

b) Tensile strains in x-direction - flexural cracks

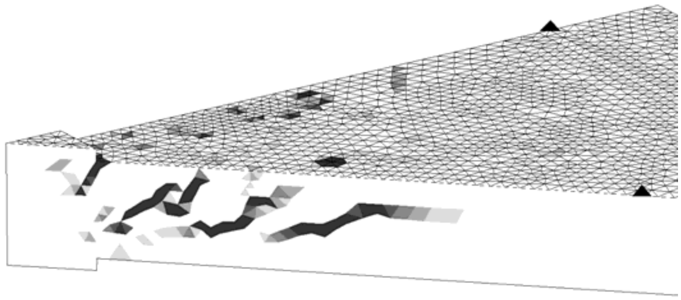

c) Tensile strains in z-direction – shear cracks
Figure 11. Cracking at ultimate load – SB4 section 2.

The crack development before ultimate load is illustrated in Figure 12. The flexural cracks at the column face and the shear cracks in the shear reinforced zone have developed. The failure crack outside the shear reinforcement is formed at ultimate load.

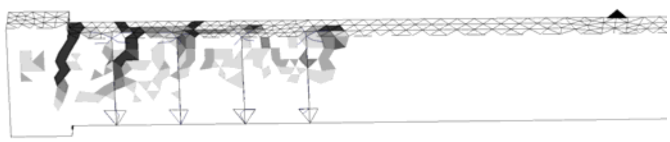

a) slab section 1

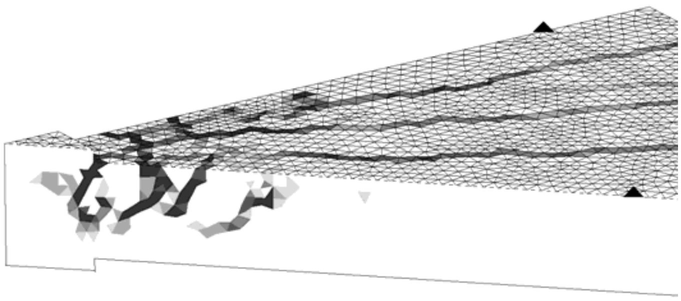

a) slab diagonal
Figure 12. Cracking at 80% of ultimate load , SB4.

4.6 *Flexural reinforcement*

The flexural reinforcement in the tests was designed to reach yield before the shear failure occurred in the slab SB1. Figure 13 shows the good agreement of the activation of the flexural reinforcement in the test and simulation before and after reaching the yield point. In the test the strain gage was damaged when the strains reached 6.5‰, so test values for ultimate load are not comparable.

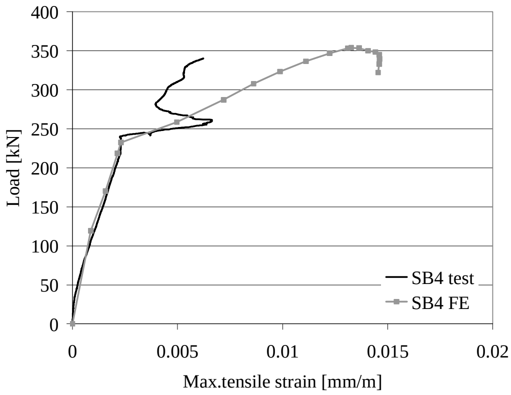

Figure 13. Flexural reinforcement strains.

4.7 *Activation of the shear reinforcement*

The activation of the shear reinforcement gives information on the formation of the shear cracks in the slab. In the punching tests, the shear bolts were very little stressed until ultimate load was reached (Figure 14 Bolt1-4). The only exception was bolt one which was subjected to small stresses at loads higher than 200 kN and was strongly activated starting at a load of 300 kN. The beginning of the bolt activations coincides with the ultimate load of a slab without shear reinforcement, SB1. This shows that shear cracking begins at the same time for slabs without and with shear reinforcements. However, the bolts can retard the opening of the shear crack considerably. Before ultimate load, the first bolt is highly stressed which shows that considerable shear cracking occurres at the column face. Furthermore the two outer rows of shear bolts are suddenly stressed at ultimate load. This shows that the shear crack outside the shear reinforcement occurs together with shear cracks that cross the outer rows of bolts.

In the simulation, the activation of all the shear bolts starts from the beginning of the slab loading were no cracking has occurred (Figure 14 FE B1-B4). This is due to the fact that the modeling of the anchorage elements of the shear bolts are connected to the concrete elements at their common nodes which allows a force transfer between them in compression and tension, while in the tests the bolt heads can only transfer load in compression. When the slab is loaded and starts deforming the part of the stud head that is away from the column face lifts from the slab surface and in the simulation tension forces in the bolts are generated. Therefore, the bolt activation alone cannot give the direct information on the crack development in the simulation. However, a stronger increase in the bolt activation shows the beginning of shear cracking as well as the shear cracking can be directly observed through the concrete strains.

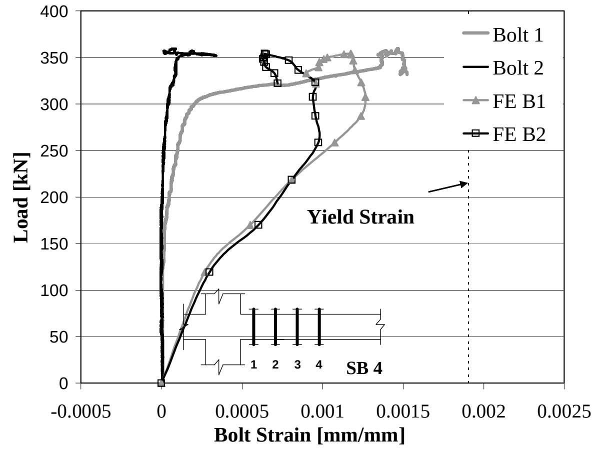

a) Bolts 1, 2

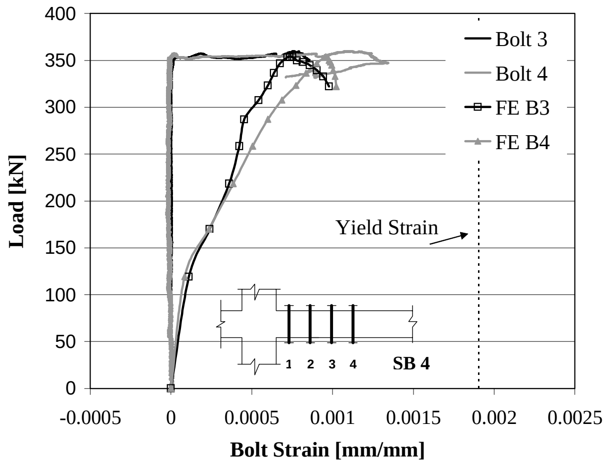

b) Bolts 3,4
Figure 14. Bolt strain for SB4.

4.8 *Summary of the finite element simulations*

The finite-element simulations show very good agreement with the test results in respect to ultimate loads, crack development and activation of the flexural reinforcement. It is clearly shown how shear bolts allow to avoid extensive shear cracking and therefore increase the punching shear load of flat slabs. From the crack development in the slab sections it can also be seen that this influence on the crack development is only valid for the regions adjacent to the shear bolts. The cracking on the slab diagonal with no shear reinforcement is almost identical to slabs without shear reinforcement. The modeling of the shear bolts and their anchorage elements is essential for the load bearing behavior of the slab. Inappropriate modeling of the anchorage elements might lead to concrete damage at the column face or no activation of the shear reinforcement which both result in ultimate loads that are too low. Even a most skillful modeling of the anchorage elements results in a bolt activation that is not entirely the same as in the tests. However, this early bolt activation can be accepted as long as the overall load bearing behavior of the slab is not negatively influenced.

5 CONCLUSIONS

The simulations of the punching tests show a good agreement with the test results. Therefore, the developed model can be used as a basis for parametric studies on the influence of the slab thickness, the reinforcement ratio and of openings in the slab adjacent to the column. The simulations can be used to gain information on the ultimate punching shear loads, the activation of the flexural reinforcement and the formation of the flexural and shear cracks.

REFERENCES

Adetifa, B., Polak, M. A. 2005, Retrofit of interior slab column connections for punching using shear bolts, *ACI Structural Journal* 102(2): 268-274.

Beutel, R. 2002, Durchstanzen schubbewehrter Flachdecken im Bereich von Innenstützen, *Dissertation*, RWTH Aachen.

Clauss, A.; Birkle, G.: Durchstanzen an Innenstützen – Die Auswirkung der Anordnung der Doppelkopfbolzen. In: Beiträge aus der Befestigungstechnik und dem Stahlbetonbau, *Festschrift zum 60. Geb. von Prof. Dr.-Ing. R. Eligehausen*. Stuttgart: ibidem-Verlag, 2002, S. 45-55.

Dilger, W. H., Ghali, A. 1981, Shear reinforcement for concrete slabs, *Journal of Structural Division,* ASCE, V. 107, No. ST12, 2403-2420.

El-Salakawy, E. F., Polak, M. A., Soudki, K.A., 2003, New shear strengthening technique for concrete slab-column connections, *ACI Structural Journal*, 100(3): 297-304.

Furche, J., 1994, Zum Trag- und Verformungsverhalten von Kopfbolzen bei zentrischem Zug, *Dissertation,* Universität Stuttgart.

Lettow, S. Mayer, U., Ožbolt, J., Eligehausen, R. 2004, Bond of RC memebers using nonlinear 3D FE analysis, *Proceedings of the Fifth International Conference on Fracture Mechanics of Concrete and Concrete Structures. FraMCoS 5*, Eds.: V.C. Li, C.K.Y. Leung, K.J. Willam, S.L. Billington , 12-16 April, Vail, Colorado, USA: 861-868. - ISBN 0-87031-135-2.

Lettow, S., 2006, Ein Verbundelement für nichtlineare Finite Elemente: Analysen - Anwendung auf Übergreifungsstöße, *Dissertation*, Institut für Werkstoffe im Bauwesen, Universität Stuttgart.

Ožbolt, J., Bažant, Z. P. 1996, Numerical smeared fracture analysis: Nonlocal microcrack interaction approach, *International Journal for Numerical Methods in Engineering*, Jg. 39, Nr. 4: 635-661.

Ožbolt, J.,Li, Y.-J., Kožar, I. 2001, Microplane model for concrete with relaxed kinematic constraint, *International Journal* of Solids and Structures, 38: 2683-2711.

Ožbolt, J., Mayer, U., Vocke, H., Eligehausen, R. 1999, Das FE-Programm MASA in Theorie und Anwendung, *Beton- und Stahlbetonbau*, Jg. 94, Nr. 10: 403-412.